THE GHOST COLLIDER: AN INNOVATIVE HIGGS FACTORY*

A. Hutton[1], P. Williams [2], R. Apsimon[3], B. R. Gamage[1], M. K. Joshi[3], K. Yokoya[4]
[1]Jefferson Lab, Newport News, USA
[2]STFC, Accelerator Science and Technology Centre (ASTeC), Daresbury, UK
[3]Lancaster University, Lancaster, UK
[4]KEK, Tsukuba, Japan

Abstract

The Ghost Collider is an innovative proposal for a 550 GeV centre-of-mass, 275 GeV per beam linear collider with four interaction regions, each with the design luminosity. The primary innovation is the use of "ghost bunches" containing equal numbers of electrons and positrons so they are electrically neutral. In the linacs, energy is transferred between electrons and positrons in the same bunch, decelerating one type of particle and using the energy to accelerate the other: a new class of Energy Recovery Linacs. At the interaction points, collisions between two neutral ghost bunches occurs with weakened electromagnetic interaction such as the beam-beam effect or disruption, ensuring that the particles and their energy can be recycled with minimal loss. Four "serial IPs" are incorporated, where chromatic errors produced in one IP are cancelled in the following IP. The neutral beam instability at the IP is also addressed. All interaction points have the nominal luminosity per IP of 2.8 x 10^{34} $cm^{-2}s^{-1}$ for a facility luminosity of 1.1 x10^{35} $cm^{-2}s^{-1}$ @ 100 MW electrical power for the RF systems. The result is a totally original concept for an electron-positron collider.

OVERVIEW

Two new bunch concepts are introduced and developed, both of which are electrically neutral, hence the name "Ghost Collider." Firstly, bunches within linacs contain an equal number of accelerating particles of one charge partnered with decelerating particles of the opposite charge. The bunches have no electromagnetic interaction with the linac cryomodules.

Secondly, bunches undergoing collision also have equal numbers of particles of both charges at the same energy. The bunches have little electromagnetic interaction with each other enabling recovery of both the particles and their energy.

BACKGROUND

The Ghost Collider concept grew out of two previous ideas. First, Valeri Telnov proposed a twin-axis energy recovery linac concept [1] consisting of two parallel superconducting linacs connected by RF couplers so that the fields are always equal. One linac is for acceleration, one for deceleration.

Erk Jensen suggested a different layout [2] and realized that if accelerating electrons and decelerating positrons (or vice versa) shared the same bucket, there would be no excitation of higher modes (HOMs) and no Multi-bunch Beam Break-Up (MBBU).

This differs from Telnov's proposal in that each of the four linacs is used for both acceleration and deceleration. For the same $E_{\max}$, the accelerating gradient is halved so dynamic losses are reduced by a factor 4, potentially allowing operation in CW mode. This comes at the expense of SR losses in the outer arcs at $E_{\max}/2$, which is still large, but only 1/16 of the synchrotron power at $E_{\max}$. A second variant of the Ghost Collider has been developed that eliminates these arcs, at the expense of additional length. This is described in an accompanying paper [3].

Accelerated electrons and decelerated positrons travel in the same linac and at the same phase location, so the total current is zero. Electrons are accelerated at the peak of the RF wave and positrons are decelerated. No energy is taken or added to the RF wave; the energy is transferred between the electrons and positrons – intra-bucket energy recovery – a new ERL mode.

GHOST COLLISIONS

Positrons and electrons in a single bunch can be brought into collision with positrons and electrons which are also in a single bunch; two neutral plasmas colliding so there will be little electromagnetic interaction (beam-beam effect or disruption).

This was first tried (unsuccessfully) at Orsay by the DCI Storage Ring Team [4]. This was followed by several papers showing that the plasmas are in an unstable equilibrium [5-8]. All of them considered a regime where the uncompensated disruption coefficient was high (between 5 and 10) as the beams would be dumped after collision. The Ghost Collider is aiming for a smaller uncompensated disruption coefficient because the beams will be recovered after collision. The previous work indicates that this regime should be stable, and this has been confirmed by simulation for the Ghost Collider conditions.

INTERACTION REGION DELAY CONCEPT

Electrons are injected into a bucket which accelerates the electrons; positrons are injected into the same bucket and are decelerated. Positrons are injected into a bucket $\lambda_{\text{Linac}}/2$ behind the first bucket and are accelerated; electrons are injected into the same bucket and are decelerated.

A chicane delays the electrons between the Linac and the Interaction Region by $\lambda_{\text{Linac}}/2$. The same layout is used for the other linac; collisions take place with zero crossing

* This material is based upon work supported by the U.S. Department of Energy, Office of Science, Office of Nuclear Physics under contract DE-AC05-06OR23177

angle. After collision, the electrons are sent through the opposite chicane to delay them by $\lambda_{Linac}/2$.

This requires a total of four chicanes and returns the order of the bunches to its initial state "Fig. 1". After leaving the IP, the electrons are placed in the same bucket as the low energy positrons, transferring their energy to them. This system is the interface between the linac ghost bunches and the IP ghost bunches.

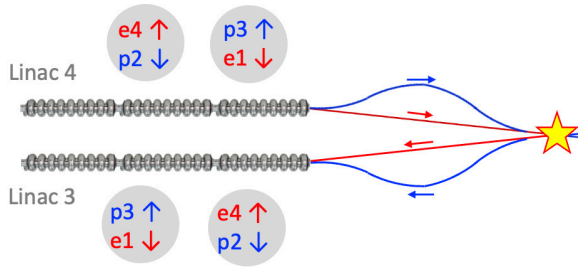

Figure 1: Ghost Collider Interaction Region showing two of four chicanes.

BEAM SHAPE AT THE INTERACTION POINT (IP)

In all linear colliders considered to date, the colliding beams are short and wide, and since the electrons and the counter-rotating positrons focus identically, both beams have the same shape at the IP. If the beams at the IP of the Ghost Collider were to follow this trend, electrons from the left against positrons from the right would also be short and wide but for electrons from the right and positrons from the left, the beam shape would be tall and thin. This shape mismatch would negate the desired compensation of electromagnetic interactions at the IP, reduce the overlap and therefore reduce the luminosity.

The best solution is to have equal horizontal and vertical emittances in all four beams and equal horizontal and vertical beta functions at the IP. All four beams will then be round and equal in size at the IP ensuring cancelation of the electromagnetic interaction.

To achieve this condition, all quadrupoles are rotated 45° throughout the Ghost Collider, including the damping rings, the linacs, the arcs and the chicanes ensuring equal horizontal and vertical emittances of the beams i.e. full transverse coupling is imposed to ensure round beams.

Triplets are used to focus the beams at the IP, rather than the usual doublets, creating equal horizontal and vertical beta functions.

COUNTER-PROPAGATION OF NEUTRAL BEAMS IN LINAC

The ghost bunches have no electromagnetic interaction with their surroundings, which enables a major simplification, a single bi-directional linac on each side of the IP. There will be head-on collisions in the linac, but the luminosity will be small with minimal loss of particles, so no bypasses are required at these locations.

However, there is an instability when the charge centres are separated, creating the equivalent of a dipole field for the incoming bunches. This is under active study including the applicability of the Bassetti-Erskin formula [9] for beams with large transverse dimensions.

To estimate the Ghost Collider luminosity and power requirements, the ILC pulsed RF parameters (1300 MHz, 31.5 MV/m, 2 K cryogenics, Q_0 = 2.7 x 10^{10}) will be adopted as they have been exhaustingly studied [10]. However, only half the ILC linac length is required which not only halves the construction cost for the cryomodules and linac tunnel but also halves the cryogenic and RF systems. When superconducting cavities with Nb_3Sn coating become available, they could be used with a corresponding decrease in cryogenic losses by a factor 3.

With a damping ring energy of 5 GeV and a top energy of 275 GeV, each linac must provide 135 GeV of acceleration. Assuming a filling factor of 71% (as in the ILC) and 10% safety factor, the two linacs, one each side of the IP, will be 5.5 km in length.

MINIMIZING ARC SYNCHROTRON RADIATION

Using the standard scaling for a storage ring, the radius of curvature should scale as the square of the energy, so the arcs in the Ghost Collider should have a radius and circumference ¼ of that of a circular collider of the same energy at the IP. For the normal design, the entry and exit to the arcs is a 60° bend of the same radius.

The circumference of each arc is then 7/6 of 2πR, and while this geometry has the shortest tunnel length, it is not necessarily the best geometry. Reducing the total bend angle reduces the synchrotron radiation but requires additional straight tunnel. The optimum shape balances reduced arc length and increased total tunnel length. The improved Arc geometry is shown in Fig. 2.

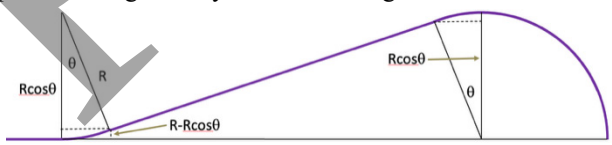

Figure 2: Improved Arc Geometry.

The shape with the arc bending angle of 22.5° seems optimum. The radius of curvature of the arc, R, is a variable to be determined by a cost optimization. The total arc length is 64.2% of the normal design, which reduces synchrotron radiation by 35.8%. The synchrotron radiation is 75% of a circular ring with same arc radius R. However, the total length is 24.7% longer than normal design with the straight section length of 2.215 R.

In the following sections, the LEP radius of curvature will be adopted, R = 3500 m, with bending radius ρ = 3,096 m and a filling factor of 88%. With an injection energy of 5 GeV and a maximum energy of 275 GeV, the arc energy is 140 GeV. The synchrotron radiation loss is then 11 GeV for a full circular ring. Since each arc is ¾ of a full arc, the synchrotron radiation loss per arc is 8.24 GeV.

Electrons and positrons are counterrotating in a single vacuum chamber but are separated by establishing double-helix trajectories like those used at the Tevatron [11].

Two low-frequency RF separators are placed at each end of the regions where electrons and positrons are counterrotating. A horizontal RF separator provides a positive horizontal kick to the electrons and a negative horizontal kick to the positrons. A vertical RF separator, one quarter betatron wavelength downstream of the horizontal separator, provides a positive vertical kick to the electrons and a negative vertical kick to the positrons initiating a helical rotation of both beams. The electrical centre of the beams is in the centre of the beampipe, avoiding excitation of transverse fields. An identical pair of RF separators at the end of the beamline restores the bunches to the central trajectory (Fig. 3).

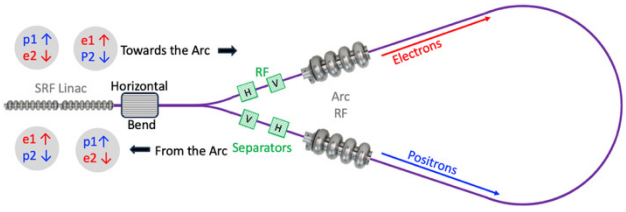

Figure 3: Linac-Arc Interface.

There is one electron bunch, e1, and one positron bunch, p1, $\lambda_{Linac}/2$ behind, accelerating into the arc coming from the damping rings. There is one positron bunch, p2, and one electron bunch, e2, $\lambda_{Linac}/2$ behind, decelerating into the arc coming from the IP superposed on e1 and p1with all the bunches having the same energy. A horizontal dipole bends the electrons left and the positrons right by an equal angle, the bunches entering the arc with electrons going clockwise, positrons counterclockwise. To avoid collisions in the arcs, helical orbits are initiated: first a horizontal RF kick followed by a vertical RF kick for the electrons $\lambda_{betatron}/2$ downstream, then a vertical RF kick followed by a horizontal RF kick for the positrons $\lambda_{betatron}/2$ downstream.

After traversing the arc, the helical orbits of the electrons and positrons are closed by the RF kickers if the distance around the arc is exactly $(n+½)\lambda_{kick}$ measured between the horizontal RF kickers or the vertical RF kickers.

The horizontal dipole again bends the electrons left and bending the positrons right, sending them both into the linac. The phases of all the bunches will be correct in the Linac if the distance around the arc measured from the centre of the last RF cell in the linac back to the centre of the last cell in the RF linac is exactly $(n+½)\ \lambda_{Linac}$.

ARC ENERGY REPLACEMENT

Both the electrons and positrons lose energy in the arcs. The two electron bunches in each arc are separated by $\lambda_{Linac}/2$ and the two positron bunches in each arc are also separated by $\lambda_{Linac}/2$. In both cases, one is going to the IR, and one is coming from the IR. Since all the bunches lose energy in the arcs, an RF system must accelerate both bunches without an energy "chirp."

The proposed solution is an RF system at 325 MHz (the fourth subharmonic of the linac frequency) plus a second harmonic RF system at 650 MHz, 180° out of phase. The disadvantage is that it takes more power: 1.33 x voltage at 325 MHz + 0.33 x voltage at 650 MHz, a total of 11 GV/arc.

The arc RF is 325 MHz with parameters of LEP scaled from 352 MHz [9]. The LEP cryomodule operates at 7.5 MV/m, providing 102 MV per cryomodule with $Q_0 = 3 \times 10^9$ @ 4.5 K, 12 m long and with a filling factor of 80%. The 650MHz cryomodules are the PIP-II high-beta design [10], operating at 18.7 MV/m providing 119 MV with a Q_0 of 3.3×10^{10} @ 2 K, and are 10 meters long.

Using the scaled LEP cavities with eight 4-cell cavities per cryomodule, the arc cryomodule has a total length of 13.9 m and the arc cryomodule energy gain is 110 MV. Each RF system requires about 50 cryomodules, which take up 695 m; the 650 MHz cavities are about 25% of this length. The total length required to accommodate each arc RF system is 6.645 km divided into two stations, one in each straight section.

THE LINAC-CHICANE INTERFACE

The linac-chicane interface is the most complex section of the Ghost Collider because on either side of the IP, there are two low-energy injected bunches and two low-energy extracted bunches which share two beamlines, two high-energy bunches going towards the IP and two high-energy bunches coming from the IP.

The low energy bunches can be extracted/injected from the linac with a simple dipole leaving the high energy particles almost unaffected (they are a factor 55 more energetic). The low-field dipole extracts electrons to the right and positrons to the left. The same magnets inject positrons from the right and electrons from the left, so helical orbits will probably be needed in the injection/extraction beamlines.

Separating the electrons and positrons going towards the IP and recombining the electrons and positrons coming from the IP requires both dipoles and RF separators.

A common RF kicker cannot deflect outgoing positrons left and incoming positrons right, so both an RF kicker and a septum magnet are required. The detailed layout of the separator/recombiner region is shown in Fig. 4.

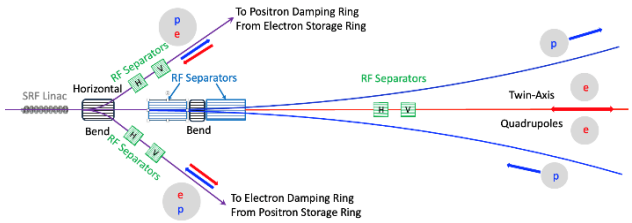

Figure 4: The Linac-Chicane Interface.

Chicanes

The chicanes delay the leading bunches so that they arrive at the IP at the same time.

Two curved beamlines are required on either side, with positrons in the curved beamlines on the left and electrons in the curved beamlines on the right. Similarly, two straight beamlines are required on either side.

The bunches all have the same energy at the end of the linacs (275 GeV), and the bunches should all have the same energy at the IP (also 275 GeV). The energy lost to synchrotron energy in the curved chicane must be replaced by RF, and the same 325 MHz cavities as the arcs will be used.

The electrons and positrons should have the same energy at the IP, independent of whether they traverse the chicane or the straight beamline, so the chicane needs an RF system to replace the synchrotron radiation loss, adding to the total length of the chicane.

The design value chosen is R = 12 km, with a total chicane length of 2 km and the synchrotron radiation loss per curved chicane = 1 GeV. The bending field is 1.54 T, well within the capability of warm dipole magnets. Note that electrons and positrons only traverse one curved chicane, either before or after collision.

Interaction Regions and Interaction Points

Electrons and positrons arrive at the IR from both directions, focused by the same IR quads. The optimum solution is to have equal transverse beta values at the IP, which requires IP final focus triplet quadrupoles. The horizontal and vertical beta values adopted at the IP are $\beta_x^* = \beta_y^* = 2$ mm (for the ILC, $\beta_x^* = 11$, $\beta_y^* = 0.48$ [11]). The transverse emittances should also be equal, and this is nearly true. The difference is that on either side of the IP, electrons and positrons either travel through a curved beamline with synchrotron radiation excitation or through a straight beamline, leading to a small emittance difference.

The Ghost bunches are not appreciably disrupted by the beam-beam collisions at the IP, which allows two or more IPs in series, one behind the other with the luminosities being additive, not shared.

The criteria for the beam separation between the IPs is that there is a –J matrix (nπ ± ½ betatron wavelengths) between the two IPs so chromatic errors cancel [12]. Cancelation removes the need for additional transverse chromatic correction of the IPs so that the beams (energy and particles) can be recovered.

A "half-IP" on either side of the IP chain creates zero chromaticity at all the IPs as shown in Fig. 5 for four serial IPs. This fully corrects the transverse chromatic effects but not the longitudinal. Various solutions are under study to correct this. There is another potential problem: a small difference in the initial position and/or angle between the centroids of the electrons and positrons in the ghost bunch leads to an increase in the separation, proportional to the disruption coefficient, limiting the maximum luminosity. This is being studied by developing the transfer matrix across the four IPs to find the maximum disruption coefficient that is stable.

The IP separation should be half the bunch spacing. In this example, n = 360 and the IP spacing is 166.14 m.

Damping Rings

The Ghost Collider has a damping ring for the positrons and either a damping ring or continuous injection for the electrons. The ILC 10 Hz Positron Damping Ring is used for both electrons and positrons for the Ghost Collider. By recycling the positrons, the requirements on a positron source are comparable to those for storage rings [13].

The Ghost Collider operates with a train of bunches separated by a delay to damp the particles. Two positron bunches and two electron bunches are extracted per collision, with 656 collisions per train. The separation between bunches in the Ghost Collider is 332.28 m or 1.11 μs, so extracting the positron and electron bunches takes 0.73 ms.

The damping ring current is 0.389 mA, the synchrotron radiation loss is 8.4 MeV/turn and assuming 50% efficiency, wall plug to RF, the electrical power required is 6.54 MW per damping ring for a total of 11.08 MW.

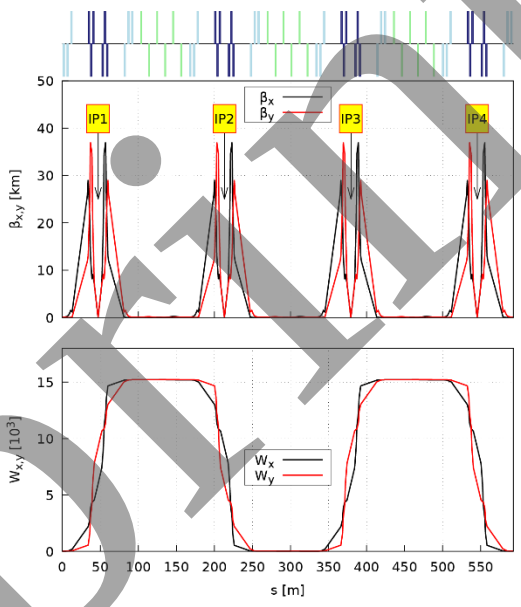

Figure 5: Four IPs – unique feature of the Ghost Collider.

Energy Spread

The energy spread squared in the linacs is reduced or increased by the ratio of the output energy to the input energy. The arc and chicane contribution to the energy spread squared is calculated using the formulae in [14]:

$$\frac{\sigma_E^2}{E^2} = 2.6\text{x}10^{-10}\,\frac{E(GeV)^5}{\rho(m)^2}\,\frac{\theta}{2\pi}$$

The normalized emittance remains constant in the linacs but is increased in the arcs and chicanes, with the increase given by the formula [14]:

$$\varepsilon_x = 1.3\text{x}10^{-10}\,\frac{E(GeV)^5}{\rho(m)^2}\langle H\rangle\,\frac{\theta}{2\pi}$$

Where $\langle H\rangle$ is approximately $\alpha R/\nu_x$. α is the momentum compaction factor, ρ is the bending radius of the ring, ν_x is the horizontal tune and $\langle H\rangle$ is the average value of H in the arcs [14].

The smallest published value of $\langle H\rangle$ is 3.3 x 10^{-5} at PETRA IV [15]; this value is used for the Ghost Collider.

The required damping is driven by the energy spread; a reduction by a factor of 6.1 is required, or about 8 ms, limiting the train repetition rate to about 120 Hz. With coupled optics, the emittance is shared between the horizontal and vertical. The horizontal and vertical emittances adopted is 6.5 mm-mrad to allow for ~10% additional blow up.

RF Power Required

The synchrotron radiation loss in each arc is 11 GeV and 1 GeV in the curved chicane beamline. The RF acceleration required from the damping rings to the IP and back to the damping rings is 23 GV. Assuming 50% efficiency wall plug to RF, the RF power required is 0.39 R MW, where R is the train repetition rate.

For the linac RF power requirements, the ILC cavities at 31.5 MV/m will be assumed. Each produces 32.75 MV, so for 135 GV per linac, 4,122 cavities are required per linac. The cavities are equipped with FE-FRTs [16] to match the power sources to the cavities. Reference [16] calculated the power required for the 1300 MHz Cornell cavities to be 365 watts so the total RF power per linac is 1.45 MW. Again assuming 50% efficiency wall plug to RF and a duty cycle of 0.73 R %, the electrical power required for both linacs is 0.042 R MW, independent of the current.

The cryogenic power is the largest contributor to the power required by the RF systems. The 1.3 GHz ILC cavity has an R/Q of 1,036 Ohm and a cavity length of 1.04 m.

With an accelerating gradient G of 31.5 MeV/m and a Q_0 of 2.7×10^{10}, the thermal dissipation $P_{\text{diss}} = 12.1$ W/cavity in CW operation. For the 4,122 cavities per linac in the Ghost Collider, the total power dissipated at 2 K for the two linacs is 73 R W. The wall power for both linacs is 0.66 R MW for a cryogenic efficiency of 900 watts /watt.

The total power required for the RF systems is plotted in Fig. 6 as a function of R.

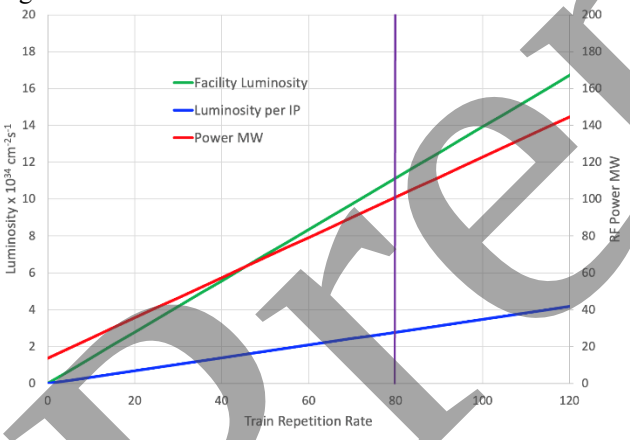

Figure 6: Luminosity per IP and the Facility Luminosity as a Function of the Train Repetition Rate.

Luminosity

The luminosity per bunch crossing is given by

$$L_b = \frac{N^2}{4\pi\sigma_x\sigma_y}$$

Where N is the number of particles in a bunch, assumed equal for electrons and positrons, f is the revolution frequency, and σ_x and σ_y are the beam sizes at the interaction point. Using the previous values: $\beta_x^* = \beta_y^* = 2$ mm; $\gamma\varepsilon_x = \gamma\varepsilon_y = 6.5$ mm-mrad, $\sigma_x\sigma_y = 2.4 \times 10^{-14}$ m^2 and finally $L_b = 5.3 \times 10^{29}$ cm^{-2}.

This should be compared with the luminosity per bunch of the ILC = 1.42×10^{30} cm^{-2}, larger by a factor of 2.7 due to the smaller beam size and the luminosity enhancement due to beam-beam disruption in the ILC.

The luminosity per IP is the product of the bunch luminosity and the bunch repetition frequency, so the luminosity per IP = 3.48×10^{32} R cm^{-2}s^{-1}.

There are four IPs and the luminosity is additive, not shared, so the facility luminosity is 1.39×10^{33} R cm^{-2}s^{-1}. Figure 5 shows the luminosity per IP and the facility luminosity as a function of R.

The luminosity per IP is 2.8×10^{34} cm^{-2}s^{-1} for an RF power of 100 MW at a train repetition rate of 80 trains/second. The facility luminosity is 11.1×10^{34} cm^{-2}s^{-1} for an RF power of 100 MW.

CONCLUSIONS

The Ghost Collider is a viable Higgs Factory, meeting the requirements of the Linear Collider vision statement.

Neutral bunches of electrons and positrons travel together in the same Linac buckets with no excitation of higher modes (HOMs) or Multi-bunch Beam Break-Up (MBBU).

There is a single, bidirectional linac, half the length of the ILC on either side of the IR region. with pulsed RF.

The arcs are a new shape, reducing synchrotron radiation by 35.8%. Two or four interaction points are possible, all with the nominal luminosity per IP of 2.8×10^{34} cm^{-2}s^{-1} @ 100 MW electrical power for the RF systems. The facility luminosity is 1.1×10^{35} cm^{-2}s^{-1}, also for 100 MW RF power.

Proof of principle solutions have been worked out for all the major components, but detailed optimization is required to validate the design.

ACKNOWLEDGEMENTS

The authors would like to thank Todd Satogata and Balša Terzić for their support and helpful insights.

REFERENCES

[1] V. Telnov, "A high-luminosity superconducting twin e⁻e⁻ linear collider with energy recovery", *J. Instrum.*, vol. 16, p. 12025, Dec. 2021. doi:10.1088/1748-0221/16/12/P125025

[2] E. Jensen, "Energy Recovery & Sustainability", presented at Symposium on Energy Recovery Linacs, June 2021. https://indico.cern.ch/event/1040671/contributions/4371231/attachments/2258316/3834416/Energy%20Recovery%20&%20Sustainability.pdf

[3] P. Williams, *et al.*, "The Linear Ghost Collider: An Efficient Higgs Factory", presented at IPAC'26, Deauville, France, May 2026, paper MOP1022, this conference.

[4] The Orsay Storage Ring Group, "Status Report on D.C.I.", *IEEE Trans. Nucl. Sci.*, vol. 26, no. 3, pp. 3559-3561, June 1979. doi:10.1109/TNS.1979.4330099

[5] V. E. Balakin and N. A. Solyak, "VLEPP: Beam-Beam Effects," SLAC National Accelerator Laboratory, Menlo Park, CA, USA, Rep. SLAC-TRANS-0226, Aug. 1986.

[6] D. H. Whittum and R. H. Siemann, "Neutral Beam Collisions at 5 TeV," SLAC National Accelerator

Laboratory, Menlo Park, CA, USA, Rep. SLAC-PUB-7808, Apr. 1986.

[7] J. B. Rosenzweig, B. Autin, P. Chen, "Instability of Compensated Beam-Beam Collisions", *AIP Conf. Proc.*, vol. 193, pp. 324-339, Oct. 1989. doi:10.1063/1.38740

[8] D. H. Whittum, A. M. Sessler, J. J. Stewart and S. S. Yu, "Plasma Suppression of Beamstrahlung", *Particle Accelerators,* vol. 33, pp. 89-104, Dec. 1989.

[9] M. Bassetti and G. A. Erskine, "Closed expression for the electrical field of a two-dimensional Gaussian charge", CERN, Geneva, Switzerland CERN-ISR-TH/80-06, Mar. 1980.

[10] "The International Linear Collider Technical Design Report", T. Behnke, Ed., CERN, Geneva, Switzerland, Jun. 2013. 11 June 2013. https://linearcollider.org/files/images/pdf/Executive%20Summary.pdf

[11] G. P. Goderre and E. Malamud, "Helical Orbit Studies in the Tevatron", in *Proc. PAC'89*, Chicago, IL, USA, Mar. 1989, pp. 1818-1821.

[12] B. Gamage and A. Hutton, "Multiple interaction points in ghost collisions", in *Proc. NAPAC'25*, Sacramento, California, USA, Aug. 2025, pp. 529-532. doi:10.18429/JACoW-NAPAC2025-TUP070

[13] F. Zimmermann, *et al.*, "Power Budgets and Performance Considerations for Future Higgs Factories", in *Proc. eeFACT'22*, Frascati, Italy, Sep. 2022, pp. 256-261. doi:10.18429/JACoW-eeFACT2022-FRXAS0101

[14] M. Sands, "The Physics of Electron Storage Rings: An Introduction", *Conf. Proc. C*, vol. 6906161, pp. 257-441, 1969. osti.gov/servlets/purl/4064201/

[15] C. G. Schroer, *et al.*, "PETRA IV: the ultralow-emittance source project at DESY", *J. Synchrotron Radiat.*, vol. 25, no. 5, pp. 1277-1290, Aug. 2018. doi:10.1107/S1600577518008858

[16] N. C. Shipman *et al.*, "A Ferroelectric Fast Reactive Tuner (FE-FRT) to Combat Microphonics", in *Proc. ERL'19*, Berlin, Germany, Sep. 2019, pp. 42-47. doi:10.18429/JACoW-ERL2019-TUCOZBS02